

# ELECTRO-OPTICAL CHARACTERISTICS OF A LIQUID CRYSTAL LENS WITH POLYMER NETWORK

S.P. BIELYKH,<sup>1</sup> S.L. SUBOTA,<sup>1</sup> V.Y. RESHETNYAK,<sup>1</sup> T. GALSTIAN<sup>2</sup>

<sup>1</sup>Taras Shevchenko National University of Kyiv, Faculty of Physics  
(2, Academician Glushkov Prosp., Kyiv 03680, Ukraine; e-mail: sveta\_pavl@ukr.net)

<sup>2</sup>Center for Optics, Photonics and Laser, Physics department, Laval University  
(Pavillon d'Optique-Photonique, 2375 Rue de la Terrasse, Quebec, Canada G1V 0A6)

PACS 42.70.Df, 61.30.Gd,  
42.15.Dp, 42.15.Fr  
©2010

We study a tunable-focus lens in which the key element is a gradient-polymer-stabilized liquid crystal (G-PSLC) structure. In this paper, we further develop the theoretical model [1, 2] that describes the dependence of the G-PSLC lens' focal length on the applied voltage and presents a theoretical study of lens aberrations. According to Fermat's principle, we minimize the optical path of a test light beam and calculate the angles of a ray exiting from the cell. Using these results, the lateral and longitudinal aberrations are estimated. The obtained results can be used to optimize the G-PSLC lenses.

## 1. Introduction

Adaptive imaging elements are more and more required for a broad range of applications, from astrophysics to security. Variable optical power is one of the key elements in such applications. In recent years, there has been much interest in lenses with variable focal length, based on liquid crystals [1–8]. These lenses are of various types and are made using manifold methods. For example, among them, there are the lenses that are created by using electrodes with holes [3] or by non-planar electrodes [4]; lenses employing Fresnel zones [5]; gradient-polymer-stabilized liquid crystal (G-PSLC) lenses [6–8], and others. But the operation of all these lenses is based on the electrical control over the refractive index distribution in a thin layer of Nematic Liquid Crystal (NLC).

In this paper, we present a theoretical model of the G-PSLC lens [1] and describe its spherical aberrations. The essence of the idea to create such a lens is the following [6, 7]. The illumination of the mixture of a planar pre-oriented NLC containing few percent up to 3% wt) of a photopolymerizable monomer by a laser beam with the Gaussian spatial intensity distribution may induce an inhomogeneous polymer network. The electro-optical response of this system to a uniform electric field is inhomogeneous, but centrally symmetric. The refractive index lateral profile is defined by the spatial distribution

of the director (the average orientation of long molecular axes of the NLC). Such a cell represents a liquid crystal lens. A change of the applied voltage varies the profile of the refractive index and, hence, controls the focal length of the lens.

The paper is organized as follows. In the first section, we describe the cell geometry of the problem, find the director reorientation under the action of an externally applied voltage in the cell with a non-uniform polymer network and the focal length of the corresponding lens. In the second section, we study the spherical longitudinal and lateral aberrations of the lens. Finally, we draw some conclusions.

## 2. Director Reorientation in the Cell with a Polymer Network Under the Action of an Externally Applied Voltage

Let us consider a NLC cell of the thickness  $L$  with planar and uniform boundary conditions at each wall. The geometry of the problem is shown in Fig. 1. We assume that there is a strong director anchoring at the cell walls. The cell is illuminated by a photopolymerizing laser beam, the intensity distribution of which is

$$I(\rho) = I_0 \exp(-\alpha\rho^2), \quad (1)$$

where we denote  $\alpha = \frac{1}{2\varpi^2}$ , and  $\varpi$  is a half-width of the Gaussian beam.

We can analyze this system when the polymerization process is over in the cell. We assume there is no significant light attenuation (due to the absorption or scattering) through the cell during the polymerization process, and the light profile is not changed noticeably. This assumption is supported by the experimental observation of a rather good fidelity of the phase profile due to the obtained gradient of the polymer network and of the spatial distribution of the polymerizing light intensity [7]. DC electric field may be applied across the cell (along

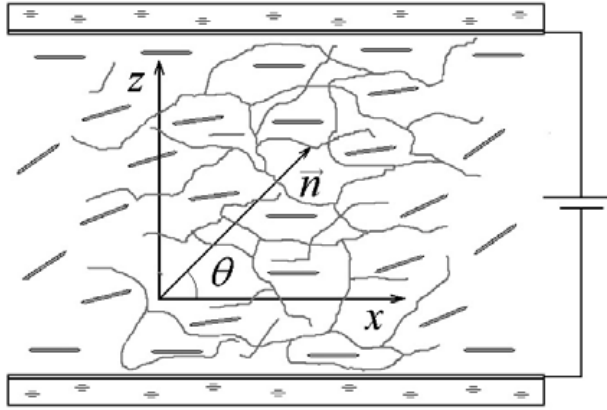


Fig. 1. LC cell geometry

the  $OZ$ -axis) by means of transparent electrodes, e.g., Indium Tin Oxide (ITO). That field would reorient the director only in the  $xz$ -plane. The obtained refractive index profile varies, as the field is applied and induces a lens-like behavior (thanks to the corresponding gradient of the polymer network), so the focal length and aberrations are also field-dependent.

From the symmetry reason, the director field is given by

$$\mathbf{n} = (\cos \theta(\rho, z), 0, \sin \theta(\rho, z)). \quad (2)$$

In order to investigate the director reorientation in the electrical field, we minimize the free energy

$$F_{el} = \frac{1}{2} \int K_1 (\nabla \mathbf{n})^2 dV + \frac{1}{2} \int K_2 (\nabla \times \mathbf{n})^2 dV + \frac{1}{2} \int K_3 (\mathbf{n} \times \nabla \times \mathbf{n})^2 dV - \frac{W}{2} \int N_p(\rho) (\mathbf{n}\mathbf{e})^2 dS - \frac{1}{2} \int \mathbf{D}\mathbf{E} dV. \quad (3)$$

The first three terms of this equation represent the usual elastic deformation contribution to the LC total free energy; in the fourth term,  $N_p$  is the density of the polymer network,  $W$  is the anchoring energy between the polymer and a liquid crystal, and  $\mathbf{e}$  is the direction of the easy axis at the bottom substrate. In the last term,  $\mathbf{D}$  is the electric displacement vector,  $K_1$ ,  $K_2$ , and  $K_3$  are the elastic constants of the pure LC, and  $N_p$  is a term whose microscopic investigation is a rather complicated task and requires a separate study. To obtain polymer network's

profile, we should solve the rate equations of chemical reactions. This task is quite complicated. To simplify this problem, we introduce a new parameter  $w = WN_p$ , representing the local effective bulk anchoring energy per unit volume. The magnitude of the parameter  $w$  can be directly determined from an experiment.

We assume that NLC is the ideal dielectric. Since the characteristic length of the director inhomogeneity in the  $z$ -direction is determined by the cell thickness, and it is much less than the characteristic size of the director inhomogeneity in the  $x$ -direction, we neglect the derivative  $\frac{\partial}{\partial \rho}$  in comparison with the derivative  $\frac{\partial}{\partial z}$ . Using the solution of the equation  $\frac{\partial D_z}{\partial z} = 0$  and combining it with the equation  $\nabla \times \mathbf{E} = 0$  with the boundary conditions  $E_x = E_y = 0$  at the cell walls, we obtain the voltage  $U$  across the nematic cell as

$$U = \int_0^L E dz = D_z \int_0^L (\varepsilon_{\perp} + \varepsilon_{\alpha} \sin^2 \theta(z))^{-1} dz. \quad (4)$$

The thermodynamic functional then takes the form

$$F = \frac{K}{2} \int [(\theta_z)^2 + (\theta_{\rho})^2] dV - \frac{W}{2} \int N_p(\rho) (\cos \theta(\rho, z))^2 dV - \frac{1}{2} \int D_z^2 (\varepsilon_{\perp} + \varepsilon_{\alpha} \sin^2 \theta(z))^{-1} dV. \quad (5)$$

Here, we used the one elastic constant approximation:  $K_1 = K_2 = K_3 = K$ .

By minimizing functional (5), we get the Euler-Lagrange equation with boundary conditions [1]

$$\left\{ \begin{aligned} &\theta''_{uu} - \frac{w(\nu)L^2}{Kb^2} \sin \theta \cos \theta + \frac{D_z^2 L^2 \varepsilon_{\alpha}}{K(\varepsilon_{\perp})^2 b^2} \frac{\sin \theta \cos \theta}{\left(1 + \frac{\varepsilon_{\alpha}}{\varepsilon_{\perp}} \sin^2 \theta\right)^2} = 0, \\ &\theta(u = 0, \nu) = 0, \\ &\theta(u = b, \nu) = 0. \end{aligned} \right. \quad (6)$$

Here, we introduced the dimensionless parameters  $\nu = \rho/L$  and  $u = \frac{z}{L}b$ ,  $b = 200$  is a scale coefficient. System (6) was solved numerically.

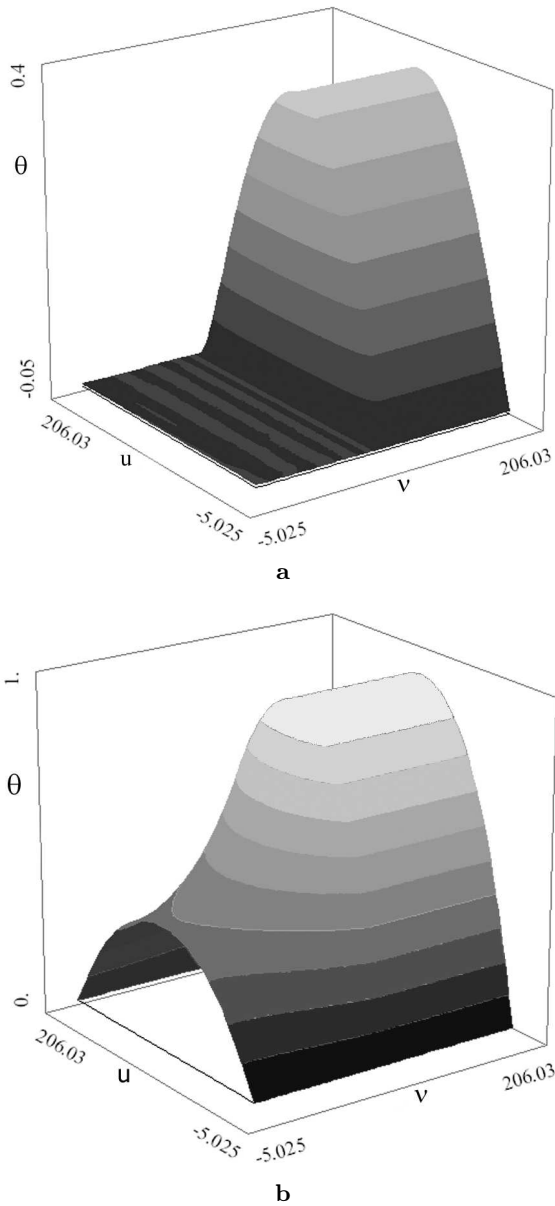


Fig. 2. Inhomogeneous director reorientation angle at dimensionless voltages  $V = 1.2$  (a) and  $V = 2.5$  (b)

As mentioned already, while considering this model, we don't consider the polymer diffusion during the polymerization process. So, we suggest that the UV light intensity profile and the polymer network's profile are of the same form. Thus, we use a Gaussian as the initial trial polymer concentration profile:

$$\tilde{w}(\nu) = w_0 \exp(-\beta L^2 \nu^2). \quad (7)$$

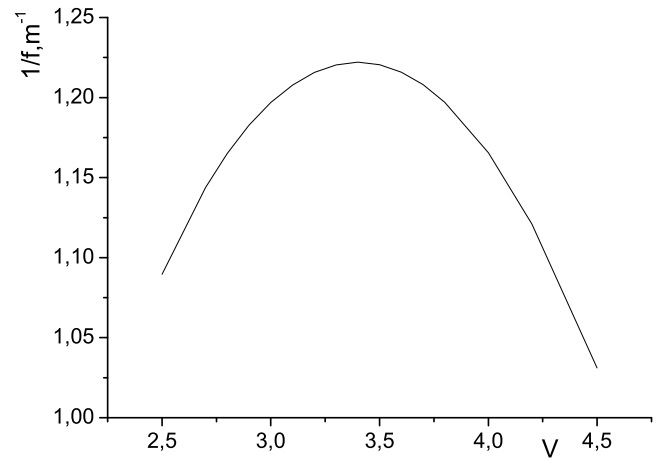


Fig. 3. Lens power dependence upon the applied voltage

In our previous theoretical work [1], we estimated a value of  $w_0 \sim 11$  using experimental data and  $\rho_0 = 90$ , where  $\rho_0$  is determined from an alternative parametrization of the polymer concentration profile

$$\begin{cases} w(\nu) = w_0(1 - \frac{\nu^2}{\rho_0^2}), & \nu \leq \rho_0, \\ 0, & \nu > \rho_0, \end{cases} \quad (8)$$

where  $\nu = \frac{\rho}{L}$ .

In this paper, we will study how the lens characteristics depend upon the dimensionless NLC-polymer anchoring interaction parameters at  $w_0 = 33$  and  $\rho_0 = 100$ .

We have solved system (6) numerically using the following parameters for the NLC mixture E7 [9] (from Merck): the principal components of the low frequency dielectric tensor  $\varepsilon_{\parallel} = 19$  and  $\varepsilon_{\perp} = 5.2$ , the principal optical refractive indices  $n_e = 1.738$  and  $n_o = 1.518$ , elastic constant  $K \approx 10^{-11}$  N, and a cell thickness  $L = 10 \mu\text{m}$ .

In Fig. 2, a and Fig. 2, b, one can see the dependences of the director reorientation angle on the coordinates of the nematic cell at some normalized voltages  $V = \frac{U}{U_0}$ , where  $U_0$  is the Frederic's threshold voltage for the pure NLC, and  $U$  is the voltage which is applied to the nematic cell.

Using the director reorientation angles and the Fresnel approximation, we obtain the lens power dependence on the applied voltage [10] (Fig. 3). Note that the obtained focal lengths have been based on the paraxial approximation. We have assumed that all rays are paraxial, that is, that they are very close to the optic axis and make very small angles with it. But this condition is never obeyed exactly. So, in the next section, we consider the aberrations of this lens.

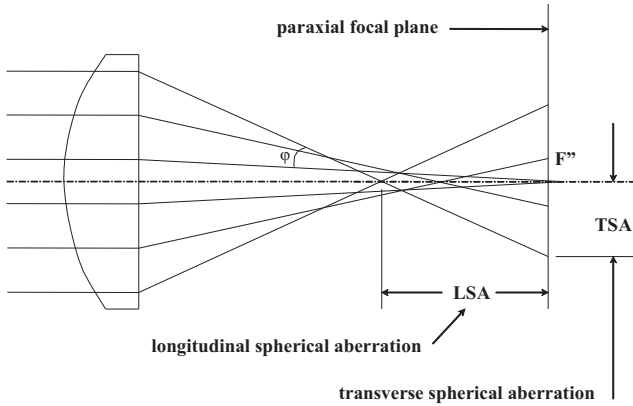


Fig. 4. Illustration of the spherical aberration

### 3. Aberration of G-PSLC Lens

In an ideal optical system, all rays of light from a point in the object plane should converge to the same point in the image plane, forming a clear image. But real optical systems, such as lenses, don't form perfect images, and there is always some degree of aberration introduced by the lens, which causes the image to be an imperfect replica of the object. The influences which cause different rays to converge to different points are called aberration. There are different types of aberration that can affect the image quality. In this paper, for the G-PSLC lens, we consider spherical ones. In Fig. 4, we show those spherical aberration definitions.

It appears from Fig. 4 that a spherically aberrated lens has no well-defined focus. Further, from the optical axis, the ray enters the lens and focuses nearer to the lens (crosses the optical axis). The distance along the optical axis between the intercept of the rays that are nearly on the optical axis (paraxial rays) and the rays that go through the edge of the lens (marginal rays) is called longitudinal spherical aberration (LSA) [11]. The height at which these rays intercept the paraxial focal plane is called transverse spherical aberration (TSA). These quantities are related by  $TSA = LSA \tan \varphi$  [12].

Theoretically, the simplest way to obtain LSA is to find the beam trajectory in an inhomogeneous liquid crystal cell. So, first we calculate the optical path length of a ray inside the layer from its entrance point *A* to its exit point *B*.

Using the eikonal equation [13]

$$(\text{grad}S)^2 = n_{\text{eff}}^2,$$

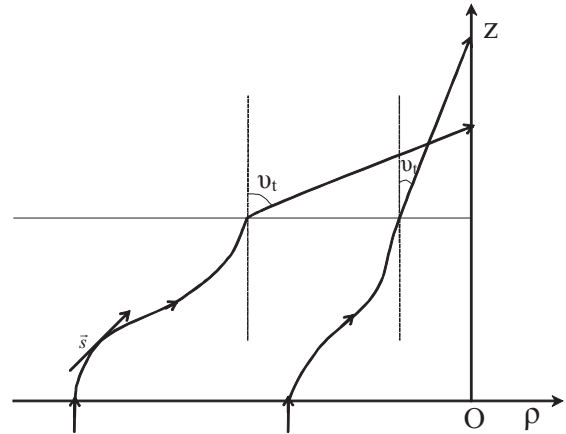


Fig. 5. Paths of two rays and the angles formed by them with the *OZ* axis

where  $n_{\text{eff}}$  is the effective refractive index given by

$$n_{\text{eff}} = \frac{n_o n_e}{\sqrt{n_e^2 \cos^2 \psi + n_o^2 \sin^2 \psi}}, \tag{9}$$

$\psi$  is the angle between the director and the wave vector inside the medium, we can write

$$\text{grad}S = n_{\text{eff}} \mathbf{s},$$

where  $\mathbf{s}$  is the unit vector directed along the propagation of the beam. Then, integrating along the beam, one can obtain the optical path length of a ray inside the layer from its entrance point *A* to its exit point *B* given by the integral

$$S = \int_A^B n_{\text{eff}} \mathbf{s} \, d\mathbf{r},$$

where  $d\mathbf{r}$  is an elementary path section along the ray. Using  $\mathbf{s}d\mathbf{r} = \cos(\phi - \vartheta)dz$ , where  $\phi = \theta + \vartheta$ ,  $\vartheta$  is the angle between *OZ* and  $\mathbf{s}$  (Fig. 5), and relation (9), we present the last integral as

$$S = n_e \int_0^L \frac{\sqrt{1 - \alpha \sin^2 \phi}}{\cos \vartheta} dz, \tag{10}$$

where  $L$  is the cell thickness, and  $\alpha = 1 - (\frac{n_o}{n_e})^2$ . According to the principle of Fermat, the actual optical path of the ray must be minimal. This means that integral (10) should be minimized. Using the Euler-Lagrange equation

$$S'_\rho - \frac{d}{dz} S'_{\rho'} = 0,$$

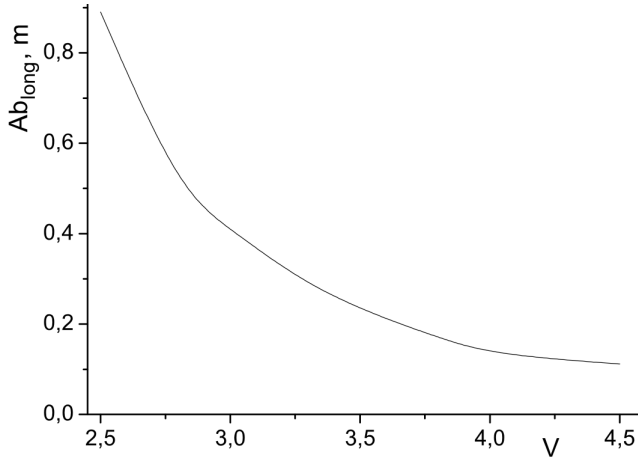


Fig. 6. Longitudinal aberration versus the applied voltage

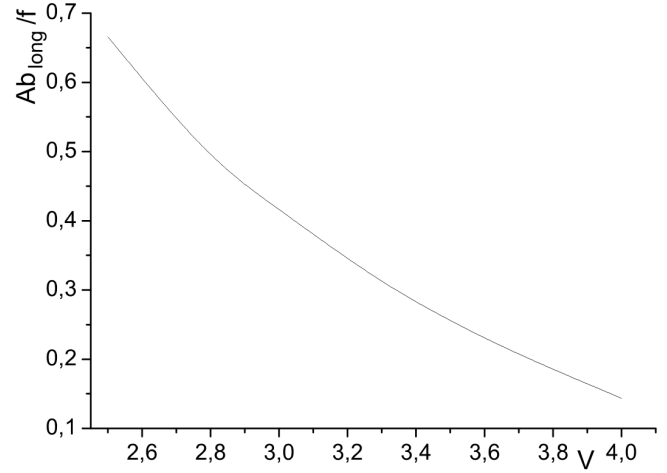


Fig. 8. Relative longitudinal aberration versus the applied voltage

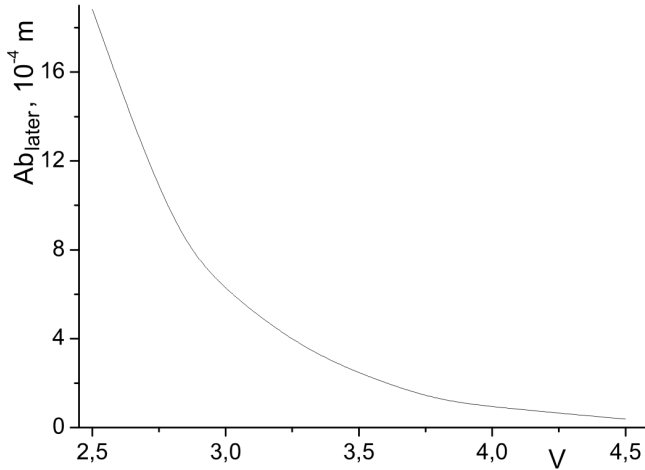


Fig. 7. Lateral aberration versus the applied voltage

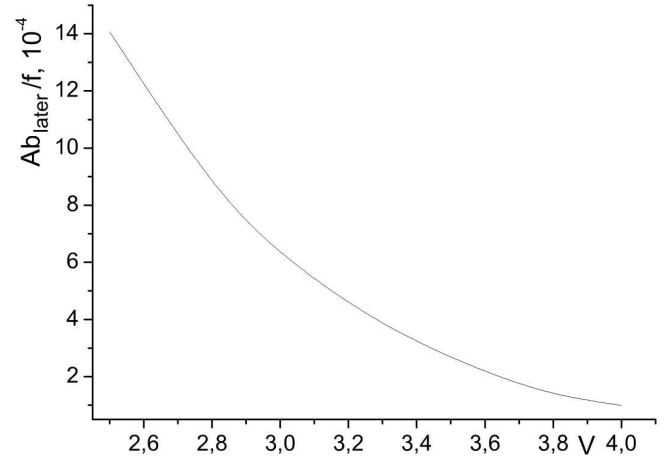


Fig. 9. Relative lateral aberration versus the applied voltage

where  $S'_\rho = -\frac{\alpha \sin 2\phi}{2g \cos 2\vartheta} \frac{\partial \theta}{\partial \rho}$ ,  $S'_{\rho'} = \frac{1}{\sqrt{1+(\rho')^2}} [\rho' g - \frac{\alpha \sin 2\phi}{2g}]$ ,  $\frac{d}{dz} S'_{\rho'} = -\theta'' \tan \theta \cos^3 \theta$ ,  $g = \sqrt{1 - \alpha \sin^2 \phi}$ ,  $\tan \theta = \frac{d\rho}{dz}$ , we can find the equation of the actual ray [14]

$$\rho'' = \frac{1}{\cos^2 \vartheta} \frac{g^3}{1-\alpha} \left\{ \left[ \left( g - \frac{1-\alpha}{g^3} \right) \tan \vartheta - \frac{\alpha \sin 2\phi}{2g} \right] \frac{\partial \theta}{\partial \rho} + \left[ g - \frac{1-\alpha}{g^3} + \frac{\alpha \sin 2\phi}{2g} \tan \vartheta \right] \frac{\partial \theta}{\partial z} \right\}. \quad (11)$$

After these lengthy calculations, we find the angle  $\vartheta_t$  of the beam propagation after the liquid crystal cell, using the Snell law for the wave vector  $\mathbf{k}$ , and then obtain lens aberrations.

Figures 6 and 7 show the expected LSA (longitudinal aberrations) and TSA (lateral aberrations) dependences on the applied voltage for  $\rho_o = 100$  and  $w = 33$ .

On the next plots, we show the dependence of relative aberrations of the G-PSLC lens on the applied voltage (Figs. 8 and 9).

#### 4. Conclusions

In this paper, we present a theoretical model that describes the electro-optical characteristic of an NLC lens based on the G-PSLC concept. We calculated the director profile of the NLC in a cell for some parameters of the lens, particularly for the Gaussian beam profile of a polymerizing beam. Using the geometric optics approximation, we found the optical path

of a ray inside the NLC in the cell. According to Fermat's principle, we minimized the functional describing the optical path of a ray and calculated angles of the ray exiting from the cell. Using these results, the lateral and longitudinal aberrations were estimated. While the optical power of the lens first goes up, the focal length and aberrations of the G-PSLC further decrease with increase in the applied voltage (for the given case of a Gaussian profile of the network). The obtained aberration and the focal length dependence on the applied voltage allows optimizing the lens parameter (including the polymer network's profile) to get the best image quality, for example, the highest optical power at the lowest aberrations. The obtained results can be applied to develop G-PSLC lenses that have no moving parts and allow the electro-optical zooming of high quality. The corresponding experiments are under way to validate the above predictions.

We acknowledge the NATO grant CBP.NUKR.CLG.981968. We are grateful to Timothy J. Sluckin (Southampton, UK) for fruitful discussions.

1. S.L. Subota, V.Yu. Reshetnyak, S.P. Pavliuchenko, and T. Sluckin, *Mol. Cryst. Liq. Cryst.* **489**, 40 (2008).
2. V.Yu. Reshetnyak, S.L. Subota, and T.V. Galstian, *Mol. Cryst. Liq. Cryst.* **454**, 187/[589]-200/[602] (2006).
3. F. Naumov, G.D. Love, M.Yu. Loktev, and F.L. Vladimirov, *Optics Express* **4**, 344 (1999).
4. B. Wang, M.Ye, M. Honma, T. Nose, and S. Sato, *Jpn. J. Appl. Phys.* **41**, L 1232 (2002).
5. Y.-H. Fan, H. Ren, and S.-T. Wu, *Optics Express* **11**, 3080 (2003).
6. V. Presnyakov and T. Galstian, *Polymer stabilized liquid crystal lens for electro-optical zoom*, *Centre for Optics, Photonics and Lasers* (Universite Laval, Quebec, Canada, 1997).
7. V. Presnyakov and T. Galstian, in *Photonics North 2004: Optical Components and Devices*, edited by J.C. Armitage, S. Favard, R.A. Lessard, G.A. Lampropoulos (2004), p. 861.
8. V.Y. Reshetnyak, S.M. Shelestiuk, S.L. Subota, S. Pavliuchenko, and T.J. Sluckin, *Theoretical modeling of heterogeneous LC systems: nano-suspensions and polymer stabilized LC lens*, 103101-1-103101-6 (2007).
9. P.S. Drzaic and A. Muller, *Liq. Cryst.* **5**, 1467 (1989).
10. J.W. Goodman, *Introduction to Fourier Optics* (McGraw-Hill, New York, 2002).
11. M. Born and E.W. Wolf, *Principles of Optics* (Pergamon Press, Oxford, 1991).
12. <http://www.mellesgriot.com/products/optics>.
13. Yu.A. Kravtsov and Yu.I. Orlov, *Geometrical Optics of Inhomogeneous Media* (Springer, Berlin, 1990).
14. J.A. Kosmopoulos and H.M. Zenginoglou, *Applied Optics* **26**, 1714 (1987). Oxford, Pergamon Press (1991).

Received 26.01.10

#### ЕЛЕКТРООПТИЧНІ ХАРАКТЕРИСТИКИ РІДКОКРИСТАЛІЧНОЇ ЛІНЗИ З ПОЛІМЕРНОЮ СІТКОЮ

С.П. Бєлий, С.Л. Субота, В.Ю. Решетняк, Т. Галстян

#### Резюме

У даній роботі вдосконалено теоретичну модель лінзи [1, 2], утвореної в нематичному рідкокристалічному кристалі в процесі фотополімеризації в неоднорідному світловому полі гаусового пучка. Знайдено чисельно кут переорієнтації директора нематичного рідкого кристала та фокусну відстань лінзи в залежності від величини напруги прикладеної до нематичної комірки. Використовуючи принцип Ферма, мінімізовано оптичний шлях світлового пучка, що проходить крізь утворену лінзу. Отримано напрямок поширення світла на виході з комірки, що дозволило оцінити поздовжню та поперечну аберації рідкокристалічної нематичної лінзи. Зі збільшенням прикладеної напруги, величина аберацій зменшується. Отримані в статті результати дозволяють оптимізувати якість зображення, що утворює лінза.